Journal of Mines, Metals and Fuels, *71(10): 1431-1441; 2023. DOI: 10.18311/jmmf/2023/35809*

Print ISSN : 0022-2755

Journal of Mines, Metals and Fuels

Contents available at: *www.informaticsjournals.com/index.php/jmmf*

Numerical Technique for a Darcy-Forchheimer Casson CuO-MgO/Methanol Hybrid Nanofluid Flow due to an Elongated Curved Surface with Chemical Reaction

K. R. Roopa*, P. A. Dinesh, Sweeti Yadav and M. V. Govindaraju

Department of Mathematics, M S Ramaiah Institute of Technology, Bangalore – 560 054 (Affiliated to Visvesvaraya Technological University, Belagavi – 590 018), India; krroopa870@gmal.com,dineshdpa@msrit.edu, sweetiyadav1989@gmail.com, govindarajumv@msrit.edu

Abstract

The insight of the present work is for analyzing the Darcy-Forchheimer model on energy and mass transfer fluid flow with the impact of CuO and MgO metallic nanoparticles with methanol as base fluid due to an elongated curved surface in uniform porous media numerically. For the two-dimensional physical model, the governing nonlinear coupled partial differential equations are derived with suitable boundary conditions and in turn, using appropriate similarity transformation transferred to nonlinear coupled ordinary differential equations. Runge-Kutta Felhberg (RKF) computational results are carried out using Maple software to understand the characteristics variations of momentum fluid flow, heat and mass transfer on various control non-dimensional parameters of the model viz local Reynolds number, Schmidt number, porosity and curvature parameters. The findings are shown numerically and graphically to demonstrate the performance of flow-related physical parameters on energy, velocity, and concentration patterns. Furthermore, the Nusselt number, skin friction coefficient and Sherwood number for the currently stated system are numerically computed. The Prandtl number denotes the deterioration of the temperature profile's performance. It is believed that increasing the Casson parameter value lowers the velocity field. Moreover, the concentration field declines as the Schmidt number grows. The findings are compared to previous studies which turn out to be in good accord.

Keywords: *Casson Hybrid Nanofluid, Curved Surface, Darcy Forchheimer*

1.0 Introduction

The flow over a curved elongated region plays a significant role in engineering and industrial applications like paper production, manufacture of artificial fibres, condensation process, oil recovery, polymer extrusion, wire drawing, glass blowing and many more. Choi and Eastman initiates the fluid with a nano-meter-sized solid particle as a nanofluid[1]. Metal or metallic oxide nanoparticles are mixed with the fluid to increase the thermal efficiency of common fluids, such as ethylene glycol and water. Nano fluid is used to enhance heat transmission. Because of the increased heat transfer capacity of the Brownian motion is connected with nanoparticles. Nanofluid increase fluid stability and thus reduces the cost of production so researchers find more interest in nanofluids. Hybrid nanofluids are the leading types of nanofluids formed by combining two different nanoparticles in the base fluid. The latency of nanoparticles in base fluid seems to be an effectual method to mark the amount of heat transfer. Metallic nanoparticles copper (Cu), titanium dioxide, (Ti) zinc (Zn), manganese (Mn), iron (Fe), and so on have

**Author for correspondence*

a high thermal conductivity which in turn enhances the heat transfer rate.

A. Mishra and Upreti studied the effect of thermophoresis and Brownian motion in comparison between hybrid nanofluid using the Buongiorno model[2]. Khan *et al.* investigate the oblique stagnation point flow of MWCNT and SWCNTs[3]. Wahid *et al*. scrutinize numerically the boundary layer flow and heat transfer of hybrid copper and alumina nanoparticles due to dual solution stability analysis was visible[4]. Later analysed the flow stability depends on the Eigenvalue, positive/ negative according to the disturbance that occurs in decay/growth of perturbation. Ahmed *et al*. analyze the flow of 2-D MHD using the Williamson model[5]. Kumar *et al*. examine the flow of the fluid with activation energy along chemical reaction by the KKL model[6]. Waqas *et al*. used hydro-magnetic transport of hybrid nano liquids to address the flow's thermal radiation and thermodynamic integrity and heat source/sink taken into account[7]. Sharma explored the effect of thermophoresis and the Brownian stream of gooey liquid Williamson nanofluid with the Darcy-Forchheimer stream and MHD stream[8]. N. Abbas *et al*. enhanced the hybrid fluid flow with the thermal slip of curved surface and compared their result of single-wall and multiwall carbon nanotubes using water as a base fluid[9]. Roşca and Pop portray the mass suction unsteady flow of stretching/shrinking over a curved surface[10]. Acharya addresses the impact of thermal energy on di hydrogen mono-oxide-based nanofluid and also analyses diffusivity using an active control strategy[11]. Fuzhang *et al*. emphasized heat and mass transfer of time-dependent flow of micropolar fluid along chemical reaction where the effect of Brownian motion and thermophoresis motion is added[12]. Z. Abbas *et al*. discussed the combined effect of radiation and heat generation by incorporating the slip effect over a curved stretching surface taking a uniform magnetic field[13].

Non-Newtonian fluids, such as Casson fluids, can be described best as shear-thinning fluids, with infinite viscosity at zero flow velocity, a straining pressure beyond which there is no flow and zero viscosity at no shear rates. Red sauce, honey, and haemoglobin are just a few examples of well-known liquids that have Casson fluid qualities. Casson nano-fluid is the basic liquid in Casson nanomaterials. Several articles relating to the Casson nano-fluid channel investigation have been published. Casson nano-fluid has industrial, biotechnology, and nutritional applications, including fermenting. Seadawy *et al.* mentioned the immersing non-Newtonian framework, progressed for chemical systems engineering as the tangential hyperbolic fluid approach, executed the HAM methodology, addressed the effects of the flow regulation parameters to conceptualize an entire worry of continuing paginating and concluded that the surface drag factor and convective heat for the plate are greater in scale compared to the other type of geometry[14]. Numerous applications in industries of Casson fluids are provided in references[15-18].

Darcy explained a conventional concept that depicts flow through a porous material. Nonetheless, this theory holds for assessments with lesser permeability and velocity. Adding the Forchheimer term to the study of nanofluids aims to improve the comprehension and simulation of how fluids move through porous media at the point whenever inertial effects become important. Because nanofluids can change fluid behaviour, the Forchheimer term takes into consideration non-linear effects that occur at higher flow velocities. A large group of scientific community researchers are working in the area of nanofluids to enhance the heat transfer coefficient using the Darcy Forchhmier model where porous media is tainted in consideration[19-23]. Building construction, oil recovery, nuclear reactors, drying techniques, cosmic fluid mechanics, heat exchangers, geothermal energies, chemical technology, and solar power all significantly depend on the understanding of the movement of mass and heat in fluids over a significantly expanding surface about chemical reaction impact. The unsteady MHD flow of changeable characteristics of nanofluid over a stretched sheet in the presence of heat radiation and chemical reaction is explored, as disclosed by Mjankwi *et al.*[24]. The figure depicts the point at which skin friction, mass, and heat transfer rates drop in response to increases in the porosity parameter and magnetic fields. The MHD flow of a third-grade fluid in the presence of a chemical reaction across an exponentially stretched sheet was studied by T. Hayat *et al.*[25]. Many researchers used the Darcy-Forchhemier model in their study[26-29].

The present structure, in particular, focuses on the growing heat transmission of Casson nanofluid with chemical reaction by employing a shooting technique. The usage of metallic nanoparticles with heat sink/source and chemical reaction in a Casson nanofluid that passes through curved surfaces is the study's innovative method.

According to the author, the current investigation was carried out for the first time. Understanding the flow properties and characteristics of these hybrid nanofluids is critical for the scientific community as the field of nanofluids develops.

2.0 Mathematical Formulation

An incompressible steady two-dimensional flow of a Casson fluid over an elongated curved surface is considered for the Darcy - Forchheimer model with CuO-MgO/Methanol hybrid nanoparticles for the study. The expression $U_w(s) = ae^{s/L}$ depicts exponential velocity along the stretching surface. T_w and C_w are respectively the wall temperature and concentration initially when r=0. Further, as r tends far away the boundary condition of the model infinity C_∞, T_∞ corresponds to ambient concentration and temperature respectively. The curvilinear coordinate s is normal to the flow and r is taken along the flow where v and u are components of velocity respectively. The radius R across the stretching sheet is illustrated in Figure 1. The heat absorption coefficient and first-order chemical reaction are considered.

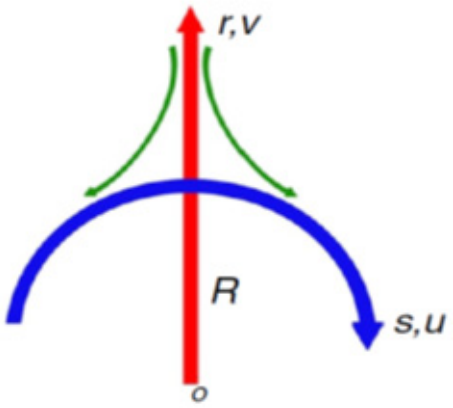

Figure 1. Physical model.

From the observation made in the physical configuration of the model, the governing equations for the model take the form of continuity, law of conservation of momentum, energy and concentration equations are given by Gohar *et al.*[30].

$$\frac{\partial}{\partial r}[(r+R)v]+\frac{\partial u}{\partial s}R=0, \tag{1}$$

$$\frac{u^2}{r+R}=\frac{1}{\rho_{hnf}}\frac{\partial p}{\partial r}, \tag{2}$$

$$v\frac{\partial u}{\partial r}+u\frac{\partial u}{\partial s}\frac{R}{r+R}+\frac{vu}{R+r}=-\frac{1}{\rho_{hnf}}\frac{\partial p}{\partial s}\frac{R}{r+R}+\nu_{hnf}\left(1+\frac{1}{\beta}\right)\left(\frac{\partial^2 u}{\partial r^2}+\frac{1}{R+r}\frac{\partial u}{\partial r}-\frac{u}{(R+r)^2}\right)-\frac{\nu_{hnf}}{K^*}u-\frac{1}{\rho_{hnf}}Fu^2, \tag{3}$$

$$\left[u\frac{\partial T}{\partial s}\frac{R}{r+R}+v\frac{\partial T}{\partial r}\right]=\alpha_{hnf}\left(\frac{\partial^2 T}{\partial r^2}+\frac{1}{r+R}\frac{\partial T}{\partial r}\right)+(T-T_\infty)\frac{Q}{(\rho c_p)_{hnf}}, \tag{4}$$

$$\left[v\frac{\partial C}{\partial r}+u\frac{\partial C}{\partial s}\frac{R}{r+R}\right]=D_{hnf}\left(\frac{\partial^2 C}{\partial r^2}+\frac{1}{r+R}\frac{\partial C}{\partial r}\right)-Kr(C-C_\infty) \tag{5}$$

Based on the base flow of the model the boundary conditions for the problem are Tasawar Hayat *et al.*[31].

$$u=U_w(s)=ae^{s/L}, \quad C=C_w=C_\infty+C_0e^{As/2L},$$
$$T=T_\infty+T_0e^{As/2L}=T_w, \quad v=0, \quad at \quad r=0$$
$$u\to 0, \quad \frac{\partial u}{\partial r}\to 0, \quad C\to C_\infty, \quad T\to T_\infty, \quad at \quad r\to\infty \tag{6}$$

Here v and u represent velocity components along s and r coordinates, ρ is the density, 'a' is the reference length, p is the pressure, L is the reference length, ν is the kinematic viscosity, and R is the radius of curvature.

$$F=\frac{C_b}{sK^{*1/2}}, \alpha=\frac{k}{(\rho c)_f}$$

F, α, K^* are the Inertia factors, thermal diffusivity and Permeability respectively.

Properties of hybrid Nanofluids are given below Tlili *et al.*[32]:

Density of the hybrid Nanofluid.

$$\frac{(\rho)_{hnf}}{(\rho)_f}=\left[1-\phi_1+\frac{\phi_1\rho_{1s}}{\rho_f}\right](1-\phi_2)+\frac{\phi_2\rho_{2s}}{\rho_f},$$

Dynamic viscosity.

$$\frac{\mu_{hnf}}{\mu_f}=(1-\phi_2)^{-5/2}/(1-\phi_1)^{5/2}, \quad \rho_{hnf}=\frac{\mu_{hnf}}{\upsilon_{hnf}},$$

Thermal conductivity of the fluid.

$$\frac{(\kappa)_{hnf}}{(\kappa)_f}=\frac{\kappa_{2s}-(\kappa_f-\kappa_{2s})2\phi_2+2\kappa_f}{\kappa_{2s}+(\kappa_f-\kappa_{2s})\phi_2+2\kappa_f}\times\frac{\kappa_{1s}-(\kappa_f-\kappa_{1s})2\phi_1+2\kappa_f}{\kappa_{1s}+(\kappa_f-\kappa_{1s})\phi_1+2\kappa_f}$$

Heat capacitance of the fluid.

$$\frac{(\rho C_p)_{hnf}}{(\rho C_p)_f}=\left[1-\phi_1+\frac{\phi_1(\rho C_p)_{1s}}{(\rho C_p)_f}\right](1-\phi_2)+\frac{\phi_2(\rho C_p)_{2s}}{(\rho C_p)_f}, \quad (7)$$

where ϕ_1 and ϕ_2 are volume frictions of CuO and MgO metallic nanoparticles.

To convert partial differential equations to ordinary differential equations, below-mentioned transformation variables are used Tasawar Hayat *et al.*[33]

$$\eta=\left(\frac{ae^{s/L}}{2\nu_f L}\right)r,\ v=-\frac{R}{r+R}\sqrt{\frac{a\nu_f e^{s/L}}{2L}}\left(f(\eta)+\eta f'(\eta)\right),$$

$$u=U_w=ae^{s/L}f'(\eta),\ p=\rho_f a^2 e^{2s/L}H(\eta)$$

$$C=C_\infty+C_0e^{As/2L}\Theta(\eta),\ T=T_\infty+T_0e^{A/2L}\Theta(\eta), \quad (8)$$

Using equation (8), equation (1) is now satisfied and equations (2), (3), (4), (5), (6) and (7) reduces to the following form

$$H'=\left(\frac{(\rho)_{hnf}}{(\rho)_f}\right)\frac{1}{\eta+k}f'^2, \quad (9)$$

$$\left(f'''+f''\frac{1}{\eta+k}-f'\frac{1}{(\eta+k)^2}-2f'\lambda\right)\left(1+\frac{1}{\beta}\right)-(1-\phi_1)^{2.5}(1-\phi_2)^{2.5}$$
$$\left(\frac{(\rho)_{hnf}}{(\rho)_f}\right)\left(k\frac{\eta+2k}{(\eta+k)^2}(f')^2-\frac{k}{\eta+k}ff''-\frac{k}{(\eta+k)^2}ff'+2Frf'^2\right)=(1-\phi_1)^{2.5}(1-\phi_2)^{2.5}\frac{k}{\eta+k}(4H+\eta H'),$$

(10)

$$\frac{k_{hnf}}{k_f}\left(\Theta''+\frac{1}{\eta+k}\Theta'\right)+\Pr\left(\frac{(\rho C_p)_{hnf}}{(\rho C_p)_f}\right)\left[\frac{k}{\eta+k}\left(f\Theta'-Af'\Theta\right)+\delta\Theta\right]=0, \quad (11)$$

$$(1-\phi_1)(1-\phi_2)\left(\Phi''+\frac{1}{\eta+k}\Phi'\right)+Sc\left(\frac{k}{\eta+k}\left(f\Phi'-f'\phi A\right)-Cr\Phi\right)=0. \quad (12)$$

Eliminating H from equation (10) using equation (9)

$$\left(1+\frac{1}{\beta}\right)\left[f^{iv}+\frac{2}{\eta+k}f'''-\frac{1}{(\eta+k)^2}f''+\frac{1}{(\eta+k)^3}f'-2\lambda\left(f''+\frac{1}{(\eta+k)}f'\right)\right]$$
$$+\frac{(\rho)_{hnf}}{(\rho)_f}\left(\frac{k}{(k+\eta)^2}f''f+\frac{k}{(k+\eta}f''f-f\frac{k}{(k+\eta)^3}f'-\frac{3k}{(k+\eta)^2}f'^2-f''\frac{3k}{(k+\eta)}f'-2F\left(2f''f'+\frac{1}{k+\eta}f'^2\right)\right)=0 \quad (13)$$

The transform conditions are given below

$$f=0,\ \Phi=1,\ f'=1,\ \Theta=1\ at\ \eta=0,\ f''\to 0,\ \phi\to 0,$$
$$f'\to 0,\ \Theta\to 0\ at\ \eta\to\infty \quad (14)$$

In the above relation, Cr is the chemical reaction, Pr is the Prandtl number, k is the curvature, Fr the Forchheimer number, Sc Schmidt number, λ the local porosity parameter, β Casson fluid, δ heat generation. This non-dimensional parameter is given by

$$Cr=\frac{2LKr}{U_w},\ \Pr=\frac{\nu_f}{\alpha_f},\ k=\left(\frac{ae^{s/L}}{2\nu_f L}\right),$$

$$\delta=\frac{2QL}{U_w(\rho c_p)},\ \lambda=\frac{\nu_f L}{K^* U_w},\ Fr=\frac{Cb}{K^{*1/2}},\ Sc=\frac{\nu_f}{D_f}, \quad (15)$$

The Sherwood Number, Skin friction, local Nusselt number, and are expressed as

$$\frac{L}{S}\left(\frac{\mathrm{Re}}{2}\right)^{-1/2}Sh_x=\Phi'(0), \quad (16)$$

$$\sqrt{\frac{\mathrm{Re}}{2}}C_{fx}=\frac{1}{(1-\phi_1)^{2.5}(1-\phi_2)^{2.5}}\left(1+\frac{1}{\beta}\right)f''(0), \quad (17)$$

$$\frac{L}{S}\left(\frac{\mathrm{Re}}{2}\right)^{-1/2}Nu_x=-\frac{k_{hnf}}{k_{bf}}\Theta'(0). \quad (18)$$

where Re_x represents the local Reynolds number

$$\mathrm{Re}_x=\frac{u_0x^2}{\nu l}, \quad (19)$$

3.0 Numerical Technique

The closed-form solutions are unattainable due to the high nonlinearity of the modified equations (11) - (13). The RKF method is used to compute these equations for different parameter estimations. In addition, the RKF approach yields good accuracy and is efficient in comparison to previous investigations. We chose this course of action for that reason. In the current study, Newton Raphson's inbuilt shooting method in Maple software is used to model the flow. The effects of increasing parameters on temperature and dimensionless velocity are examined. The step size, as the convergence criterion, is ($\Delta\eta$ = 0.01). Convergence criteria (10^6) are used in

Table 1. Physical and thermal properties Tlili *et al.*[32].

Nanomaterials and base fluid	$\rho(kg/m^3)$	$C_p(j/kgK)$	$k(W/mK)$
Methanol	792	2545	0.2035
CuO	6320	531.8	76.5
MgO	3580	960	48.4

every instance to complete the inner iteration. Table 1 lists the thermophysical characteristics of base fluids and nanoparticles. The values of Skin friction, Nusselt number(Nu) and Sherwood Number(Sh) for various values$\phi_1 = \phi_2$,A = 0.4, k = 0.6, Pr = 6.3, Fr=0.6, and λ = 0.2 are validated with the earlier established results[30] are tabulated in Table 2, and the comparison shows the good agreement. This is done to ensure the accuracy of the findings obtained by the numerical approach used in this work.

Table 2. The analysis is compared to the existing work for $\phi_1 = \phi_2$,A = 0.4, k = 0.6, Pr = 6.3, Fr=0.6,and λ = 0.2

Results	Gohar et al.[30]	present
$f''(0)$	0.7352130	0.73520294
$-\Theta'(0)$	-1.3752410	-1.328421915
$-\Phi'(0)$	-1.3620189	-1.345982203

4.0 Result and Discussion

The equations (11)-(13) are highly coupled non-linear equations hence we employ the RKF technique for better accuracy and the solutions are computed numerically using Maple. The main interest is to observe the effect of the physical parameters like Casson parameter β, Forchhemmier number Fr, curvature parameter k, Prandtl number Pr, porosity λ, Schmidt number Sc, heat absorption δ and chemical reaction parameter Cr, on concentration, temperature and velocity profile are presented in Figures (2)-(13).

Parameters influence concentration, temperature and velocity profile:

Figure 2 indicates that when the heat-generating effect increases, the ambient temperature of the tiny fluid rises slowly. This result is consistent with the idea that heat creation serves as a source of thermal energy in the flow mechanism. Figure 3 demonstrates the effect

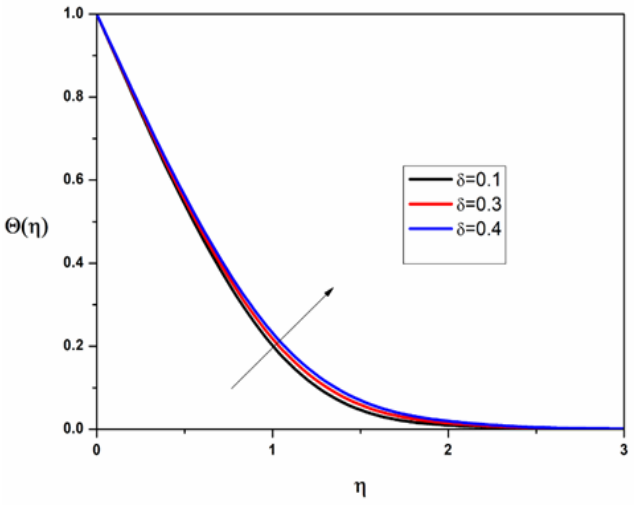

Figure 2. Influence of heat absorption on the temperature profile.

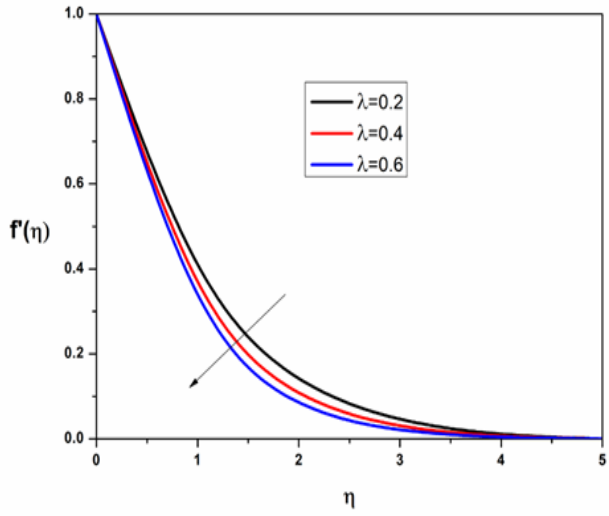

Figure 3. Influence of porosity parameter on the $f'(\eta)$.

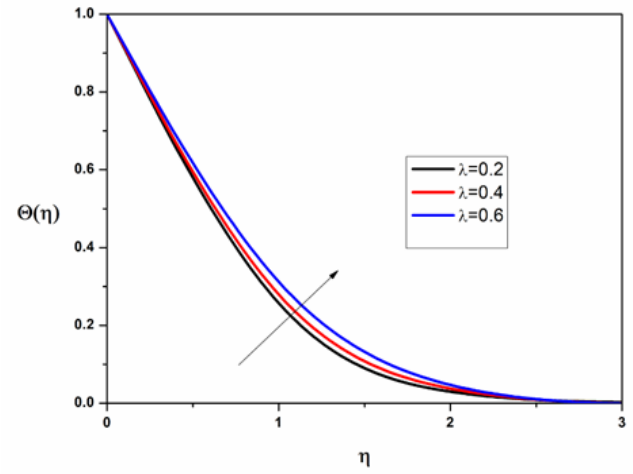

Figure 4. Influence of λ local porosity parameter on the $\Theta(\eta)$.

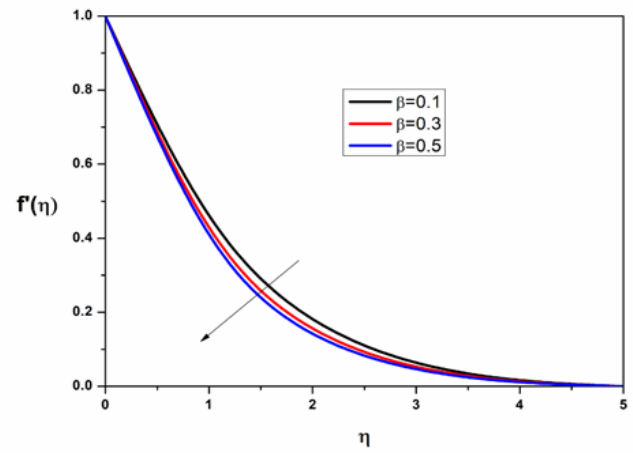

Figure 5. Impact of Casson parameter on the $f(\eta)$.

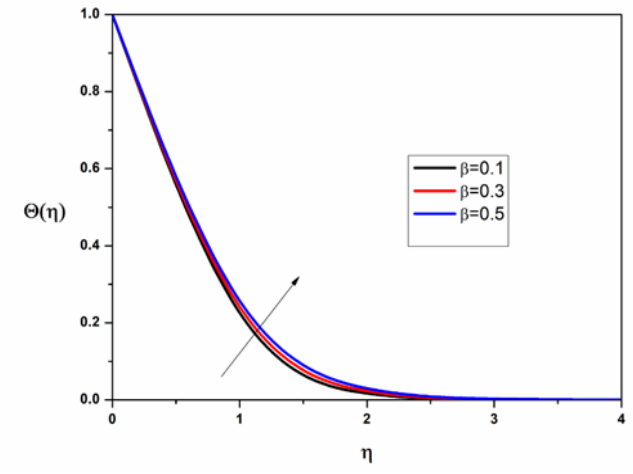

Figure 6. Control of Casson parameter on the $\Theta(\eta)$.

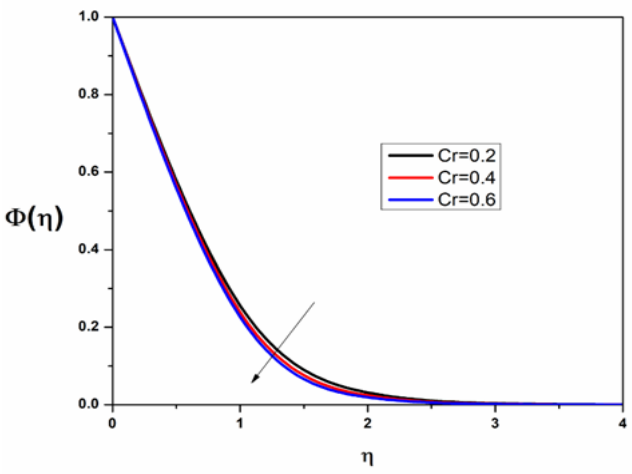

Figure 7. Influence of chemical reaction parameters on the $\Phi(\eta)$.

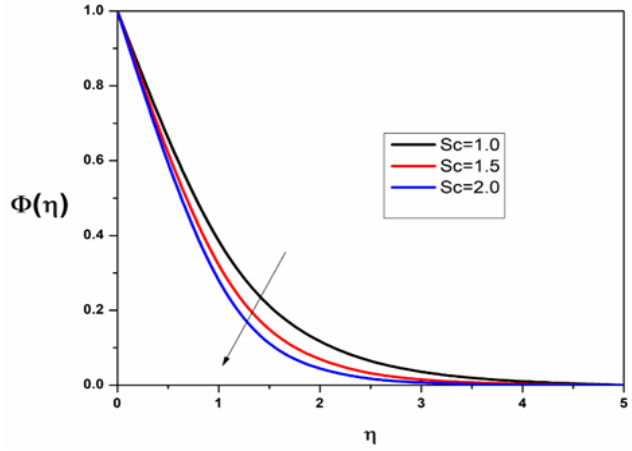

Figure 8. Influence of Schmidt parameter on the $\Phi(\eta)$

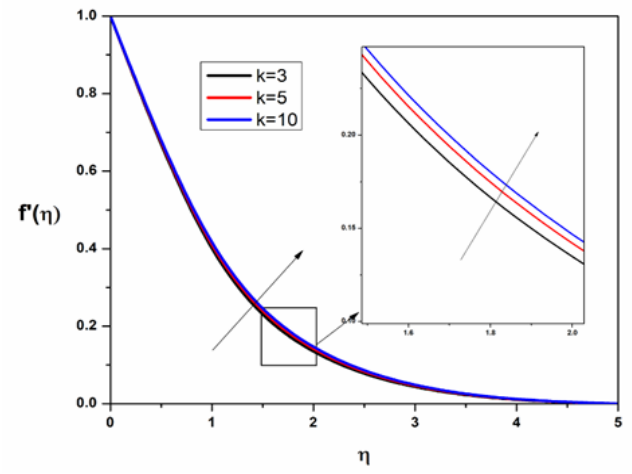

Figure 9. Influence of curvature k on the $f'(\eta)$.

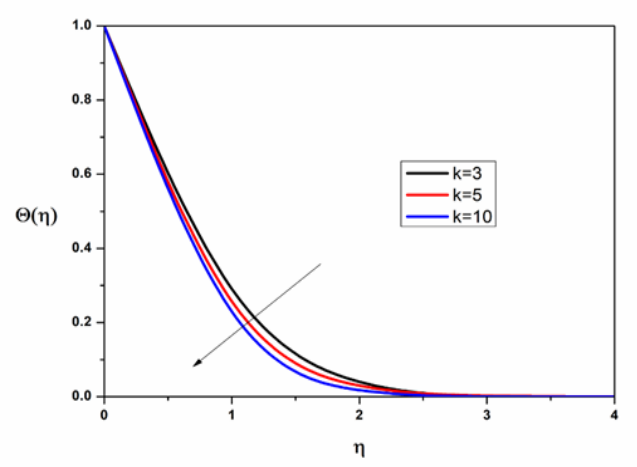

Figure 10. Influence of curvature k on the $\Theta(\eta)$.

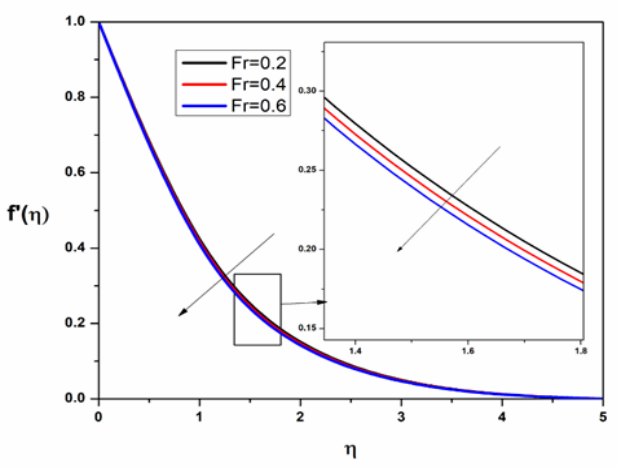

Figure 12. Impact of Forchhemier on the $f^{'}(\eta)$.

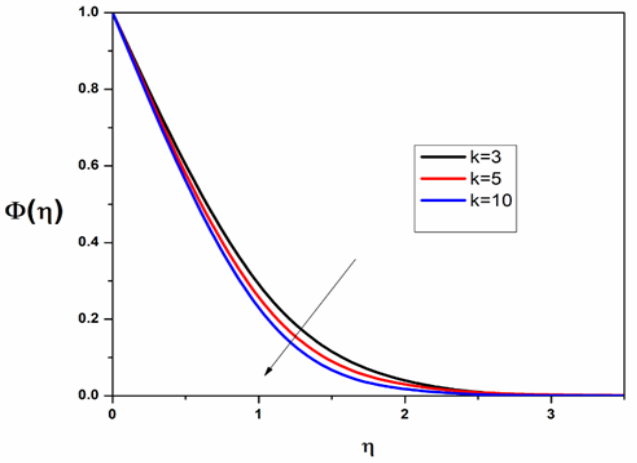

Figure 11. Impact of curvature k on the $\Phi(\eta)$.

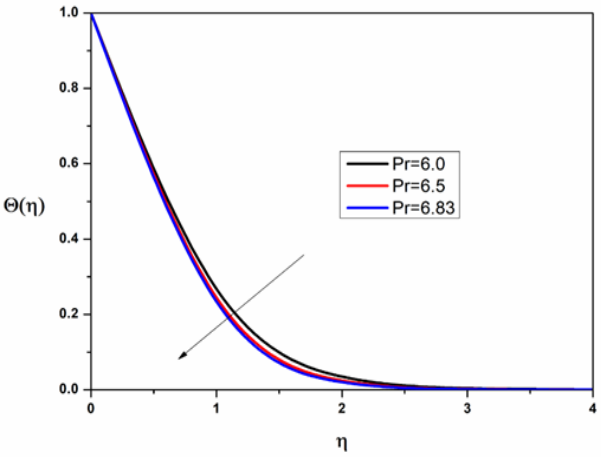

Figure 13. Impact of Prandtl on the $\Theta(\eta)$.

of the porosity parameter k on the velocity pattern. As the value of k grows, the velocity field decreases. Since the existence of a porous media increases the barrier to flow, the fluid momentum falls. Figure 4 depicts the effect of the porosity parameter k on the energy profile, and it is seen that as the porosity parameter value grows, it also increases the temperature of the fluid. As porosity is inversely proportional to permeability it enhances the resistive flow of the fluid so the velocity of the fluid will be decreased whereas temperature is increased.

Figure 5 demonstrates that when the Casson fluid parameter expands, the velocity in the boundary layer area drops. It is also revealed that raising Casson parameter b reduces velocity because greater lead levels reduce yield stress. Figure 6 shows that when the Casson fluid parameter value increases, so does the temperature within the tiny particles. The thickness of the thermal boundary layer increases as the flexibility force component increases. Figure 7 illustrates that as the chemical reaction parameter rises, the concentration of nanoparticles drops. This occurs when electrically reactive materials break down causing damage to chemical reaction mechanisms. Figure 8 visualize the features of Sc (the Schmidt number) on the mass sketch. The greater estimate of Sc is shown to decline as the particle mass and related boundary layer get thinner. Physically, when Sc increases, mass diffusivity decreases, and as an outcome, the concentration profile decreases. Variations in curvature parameters on

transport profiles are demonstrated in Figures 9-11 The velocity distributions grow as curvature increases as noted in Figure 9. In reality, the curvature factor is proportional to the radius of the curved component. As the curvature factor increased, the surface with curves became flat. An increase in curvature factor boosts velocity profiles since the profile grows faster at the flat surface rather than the curved surface. Figure 10 depicts the effects of k on the temperature profile. Greater values diminish the viscous force (i.e., kinematic viscosity decay), which correlates to the declination of energy. Fluid mobility increases when the fluid's kinematic viscosity decreases, resulting in a smaller thermal boundary layer. This results in greater convective heat transmission and increased thermal energy exchange between the fluid and the environment. As a result, the declination of curvature is definite similar behavior is found for the concentration profile in Figure 11. Figure 12 depicts the control of the Forchheimer parameter (local inertial force) on fluid velocity. Physically, the greater the barrier for the movement of fluids, the

Table 3. Numerical data for Skin friction, Nusselt number and Sherwood Numbers are tabulated.

ϕ_1	ϕ_2	λ	β	Fr	A	Cr	Pr	Sc	δ	k	$-\sqrt{\frac{\mathrm{Re}}{2}}C_{fx}$	$-\left(\frac{\mathrm{Re}}{2}\right)^{-1/2}Nu_x$	$-\left(\frac{\mathrm{Re}}{2}\right)^{-1/2}Sh_x$
0.01	0.02	0.2	0.5	0.6	0.4	0.5	6.2	3	0.5	5	1.1899872	1.24626635	2.026996008
0.02											1.183768574	2.017018497	1.241944663
	0.03										1.193039651	2.037388087	1.245982203
		0.4									1.359228283	1.216469737	2.00466622
		0.6									1.509850876	0.950965242	1.985465392
			0.1								0.928060413	1.425686373	2.05783581
			0.3								1.085435905	1.328421915	2.039056444
				0.2							1.102992146	1.310618507	2.036430384
				0.4							1.147350291	1.279531035	2.031590881
					0.3						1.1899872	1.043796321	1.964782734
					0.5						1.1899872	1.43063115	2.087955965
						0.4					1.1899872	1.24626635	1.939904936
						0.6					1.1899872	1.24626635	2.109793071
							6.5				1.18998722	1.309878757	2.026995998
							6.83				1.189987215	1.372876384	2.026996001
								1			1.1899872	1.246266351	1.143891449
								2			1.1899872	1.24626635	1.640894922
									0.1		1.189987218	2.124985599	2.026995998
									0.3		1.189987205	1.758950391	2.026996006
										5	1.1899872	1.24626635	2.026996008
										10	1.157225606	1.344240672	1.998074178

slower the flow speed reacts and the related boundary layer shrinks. Figure 13 demonstrates the importance of the energy profile. Because of the rising variation provided by Pr, the heat distribution profile decays. The percentage of thermal conductivity to diffusion coefficient ratio is represented by the Prandtl number. As a result, increasing the Prandtl number decreases thermal diffusivity. As a result, when the Prandtl number rises, the temperature profile falls.

Variations of several relevant factors on Nusselt number, Skin friction and Sherwood Number are indicated in Table 3. As volume friction parameter and curvature increase skin friction and Sherwood decline whereas heat transfer rate improves. For increased Forchhimer, Casson, heat absorption and porosity variables there is a rise in surface drag force and for other parameters it remains constant. As the chemical reaction parameter grows Sherwood's number increases, but the opposite nature is found on the Schmidt parameter.

5.0 Conclusion

The steady flow of CuO and MgO hybrid Nano fluids enhances heat and mass transfer rate due to their high thermophysical properties over an exponentially curved surface. The RKF method is employed to solve the system of nonlinear equations numerically. The results obtained are discussed through graphs and tables.

- Hybrid nanofluids have excellent thermal conductors due to their physical property it has many industrial applications like coating, geology, water purification, chemical reactors and device modelling.
- As the Casson parameter increases, the velocity flow of the nanofluids decreases as the temperature rises.
- The acceleration of nanofluids drops as the porosity parameter k rises, while the opposite is true for temperature.
- Forchhemier term delays velocity profile.
- The thermal profile reduces as the Schmidt number increases.
- The influence of Prandlt number in energy profile declines
- A decline in drag force and Sherwood for curvature variable is evident

6.0 Acknowledgement

Authors RKR and SY are grateful to the management of R.I.T, for granting with Research fellowship and for their encouragement.

7.0 References

1. Choi SUS, Eastman J. Enhancing thermal conductivity of fluids with nanoparticles, developments and applications of non-newtonian flows. ASME, New York. 1995;38.
2. Mishra A, Upreti H. A comparative study of Ag–MgO/water and Fe_3O_4–$CoFe_2O_4$/EG–water hybrid nanofluid flow over a curved surface with chemical reaction using Buongiorno model. Partial Differ Equations Appl Math. 2022 Jun 1; 5.
3. Khan MR, Pan K, Khan AU, Ullah N. Comparative study on heat transfer in CNTs-water nanofluid over a curved surface. Int Commun Heat Mass Transf. 2020 Jul 1; 116.
4. Wahid NS, Arifin NM, Khashi'ie NS, Pop I, Bachok N, Hafidzuddin MEH. Flow and heat transfer of hybrid nanofluid induced by an exponentially stretching/shrinking curved surface. Case Stud Therm Eng. 2021 Jun; 25:100982.
5. Ahmed K, Akbar T, Muhammad T, Alghamdi M. Heat transfer characteristics of MHD flow of Williamson nanofluid over an exponential permeable stretching curved surface with variable thermal conductivity. Case Stud Therm Eng. 2021 Dec 1; 28.
6. Kumar RN, Gowda RJP, Alam MM, Ahmad I, Mahrous YM, Gorji MR, *et al*. Inspection of convective heat transfer and KKL correlation for simulation of nanofluid flow over a curved stretching sheet. Int Commun Heat Mass Transf [Internet]. 2021 Jul; 126:105445. Available from: https://linkinghub.elsevier.com/retrieve/pii/S0735193321003389
7. Waqas H, Bukhari FF, Farooq U, Alqarni MS, Muhammad T. Numerical computation of melting heat transfer in nonlinear radiative flow of hybrid nanofluids due to permeable stretching curved surface. Case Stud Therm Eng. 2021 Oct 1; 27.
8. Sharma S. Study on Darcy-Forchheimer Flow and MHD Boundary Layer Flow with Heat Transfer Characteristics of Williamson Nanofluid over Curved Stretching Surface. In: Journal of Physics: Conference Series. IOP Publishing Ltd; 2021.
9. Abbas N, Rehman KU, Shatanawi W, Malik MY. Numerical study of heat transfer in hybrid nanofluid flow

over permeable nonlinear stretching curved surface with thermal slip. Int Commun Heat Mass Transf [Internet]. 2022; 135(May):106107. Available from: https://doi.org/10.1016/j.icheatmasstransfer.2022.106107

10. Roşca NC, Pop I. Unsteady boundary layer flow over a permeable curved stretching/shrinking surface. Eur J Mech B/Fluids. 2015; 51:61–7.
11. Acharya N. Active-passive controls of liquid di-hydrogen mono-oxide based nanofluidic transport over a bended surface. Int J Hydrogen Energy. 2019 Oct 18; 44(50):27600–14.
12. Fuzhang W, Anwar MI, Raza M, El-Shafay AS, Abbas N, Ali R. Inspections of unsteady micropolar nanofluid model over exponentially stretching curved surface with chemical reaction. Waves in Random and Complex Media. 2022;
13. Abbas Z, Naveed M, Sajid M. Hydromagnetic slip flow of nanofluid over a curved stretching surface with heat generation and thermal radiation. J Mol Liq. 2016 Mar 1; 215:756–62.
14. Seadawy A, Raza N, Khalil OH, Khan KA, Usman M. Computational approach and flow analysis of chemically reactive tangent hyperbolic nanofluid over a cone and plate. Waves in Random and Complex Media [Internet]. 2021 Aug 9; 1–15. Available from: https://www.tandfonline.com/doi/full/10.1080/17455030.2021.1959960
15. Mahabaleshwar US, Aly EH, Anusha T. MHD slip flow of a Casson hybrid nanofluid over a stretching/shrinking sheet with thermal radiation. Chinese J Phys. 2022 Dec 1; 80:74–106.
16. Alwawi FA, Hamarsheh AS, Alkasasbeh HT, Idris R. Mixed Convection Flow of Magnetized Casson Nanofluid over a Cylindrical Surface. Coatings [Internet]. 2022 Feb 22; 12(3):296. Available from: https://www.mdpi.com/2079-6412/12/3/296
17. Upreti H, Pandey AK, Joshi N, Makinde OD. Thermodynamics and Heat Transfer Analysis of Magnetized Casson Hybrid Nanofluid Flow via a Riga Plate with Thermal Radiation. J Comput Biophys Chem [Internet]. 2023 May 27; 22(03):321–34. Available from: https://www.worldscientific.com/doi/10.1142/S2737416523400070
18. Abbas N, Shatanawi W, Abodayeh K. Computational Analysis of MHD Nonlinear Radiation Casson Hybrid Nanofluid Flow at Vertical Stretching Sheet. Symmetry (Basel). 2022; 14(7):1–17.
19. Cui J, Jan A, Farooq U, Hussain M, Khan WA. Thermal Analysis of Radiative Darcy–Forchheimer Nanofluid Flow Across an Inclined Stretching Surface. Nanomaterials [Internet]. 2022 Dec 2; 12(23):4291. Available from: https://www.mdpi.com/2079-4991/12/23/4291
20. Rasool G, Shafiq A, Khalique CM, Zhang T. Magnetohydrodynamic Darcy–Forchheimer nanofluid flow over a nonlinear stretching sheet. Phys Scr [Internet]. 2019 Oct 1; 94(10):105221. Available from: https://iopscience.iop.org/article/10.1088/1402-4896/ab18c8
21. Jawad M, Hameed MK, Nisar KS, Majeed AH. Darcy-Forchheimer flow of maxwell nanofluid flow over a porous stretching sheet with Arrhenius activation energy and nield boundary conditions. Case Stud Therm Eng [Internet]. 2023 Apr; 44:102830. Available from: https://linkinghub.elsevier.com/retrieve/pii/S2214157X23001363
22. Muhammad T, Alsaedi A, Shehzad SA, Hayat T. A revised model for Darcy-Forchheimer flow of Maxwell nanofluid subject to convective boundary condition. Chinese J Phys. 2017 Jun; 55(3):963–76.
23. Shree VV, Rudresha C, Balaji C MS. Effect of MFD viscosity on ferroconvection in a fluid saturated porous medium with variable gravity. J Mines, Met Fuels. 2022 Jul; 1298-103.
24. Mjankwi MA, Masanja VG, Mureithi EW, James MN. Unsteady MHD Flow of Nanofluid with Variable Properties over a Stretching Sheet in the Presence of Thermal Radiation and Chemical Reaction. Int J Math Math Sci [Internet]. 2019 May 2; 2019:1–14. Available from: https://www.hindawi.com/journals/ijmms/2019/7392459/
25. Hayat T, Khan MI, Waqas M, Alsaedi A, Yasmeen T. Diffusion of chemically reactive species in third grade fluid flow over an exponentially stretching sheet considering magnetic field effects. Chinese J Chem Eng [Internet]. 2017 Mar; 25(3):257–63. Available from: https://linkinghub.elsevier.com/retrieve/pii/S1004954116303810
26. Wahida Khalili NN, Samson AA, Abdul Aziz AS, Ali ZM. Chemical reaction and radiation effects on MHD flow past an exponentially stretching sheet with heat sink. J Phys Conf Ser [Internet]. 2017 Sep; 890:012025. Available from: https://iopscience.iop.org/article/10.1088/1742-6596/890/1/012025
27. Reddy NN, Rao VS, Reddy BR. Chemical reaction impact on MHD natural convection flow through porous medium past an exponentially stretching sheet in presence of heat source/sink and viscous dissipation. Case Stud Therm Eng [Internet]. 2021 Jun; 25:100879.

Available from: https://linkinghub.elsevier.com/retrieve/pii/S2214157X21000423
28. Mishra N, Mohanmoduly M, Mohapatra NB. Effect Of Chemical Reaction On Nanofluid Flow Over An Unsteady Stretching Sheet In Presence Of Heat Source. 8(8):142–66.
29. Pandey AK, Upreti H. Mixed convective flow of Ag–H_2O magnetic nanofluid over a curved surface with volumetric heat generation and temperature-dependent viscosity. Heat Transf [Internet]. 2021 Nov 30; 50(7):7251–70. Available from: https://onlinelibrary.wiley.com/doi/10.1002/htj.22227
30. Gohar, Khan TS, Sene N, Mouldi A, Brahmia A. Heat and Mass Transfer of the Darcy-Forchheimer Casson Hybrid Nanofluid Flow due to an Extending Curved Surface. J Nanomater. 2022; 2022.
31. Hayat T, Haider F, Muhammad T, Alsaedi A. Numerical study for Darcy-Forchheimer flow of nanofluid due to an exponentially stretching curved surface. Results Phys. 2018 Mar; 8:764–71.
32. Tlili I, Nabwey HA, Samrat SP, Sandeep N. 3D MHD nonlinear radiative flow of CuO-MgO/methanol hybrid nanofluid beyond an irregular dimension surface with slip effect. Sci Rep. 2020; 10(1):1–14.
33. Hayat T, Haider F, Muhammad T, Alsaedi A. Numerical treatment for Darcy-Forchheimer flow of carbon nanotubes due to an exponentially stretching curved surface. J Cent South Univ. 2019 Apr 1; 26(4):865–72.